*Advances in Engineering Research, volume 133*
Actual Issues of Mechanical Engineering (AIME 2017)

# *Oil Separator*

Bogaudin Khamidovich Gaitov
Department of Electrical Engineering and Electrical Machines
Kuban State Technological University
Krasnodar, Russia
e-mail kkllev1@mail.ru

Yakov Mikhajlovich Kashin
Department of Electrical Engineering and Electrical Machines
Kuban State Technological University
Krasnodar, Russia
e-mail jlms@mail.ru

Lev Efimovich Kopelevich
Department of Electrical Engineering and Electrical Machines
Kuban State Technological University
Krasnodar, Russia
e-mail kkllev@mail.ru

Alexander Valeryevich Samorodov
Department of Electrical Engineering and Electrical Machines
Kuban State Technological University
Krasnodar, Russia
e-mail Alex.Samorodoff@gmail.com

Vladislav Anatolievich Kim
Department of Electrical Engineering and Electrical Machines
Kuban State Technological University
Krasnodar, Russia
e-mail vladk-kub@mail.ru

Polina Vitalievna Sereda
Department of Technical and Scientific Translation
Kuban State Technological University
Krasnodar, Russia
polinapost@list.ru

***Abstract* – The engine-separator of combined design is considered in the article. The subject of this article is temperature field investigation of the engine-separator with a combined design. The purpose of this paper is to review and analyze the application of an oil separation unit based on a separator engine at oil and gas facilities. The article describes a method for oil separation based on the use of a combined engine-separator design; the use of losses in the rotor, which is the separator drum, as "heating" losses heat during separation of product in the separator drum; the use of the energy losses released by separator engine core and stator winding for preheating the separation product. The authors studied the questions connected with construction of a temperature field of the machine in order to improve the machine design and reduce the power consumption.**

***Keywords – centrifugal separator, oil separation, engine-separator.***

## I. INTRODUCTION

Oil extracted from the earth interior contains, as a rule, a gas called by-pass gas, formation water, mineral salts, and various mechanical impurities. For each ton of oil produced, there are 50-100 $m^3$ of associated (oil) gas, 200-300 kg of water, in which the salts are dissolved. Before transportation and supply of oil for processing, the gas must be separated from oil [1]. Separation of oil from gas, called separation, is carried out in separators of different designs (horizontal, vertical, cylindrical, spherical ones, etc.). However, all separators, regardless of their design, perform certain functions, the main of which are: separation of gas from oil and separation of oil from water in the presence of unstable emulsions [2].

## II. RESULTS AND DISCUSSION

Crude oil is supplied from the group (claster) of wells to several Automatic Pad Metering Stations (APMS), which measure the production rate of each well. Then, crude oil is sent to the booster pump station (BPS) where the following production stages take place: gas separation from oil (1), preliminary separation of water (2) and mechanical impurities (3) (see figure 2). After separation of the main amount of gas, the oil containing formation water and gas residues enters the separator second stage (S-2), where most of the water and a part of the gas are separated, and water-oil emulsion is sent to the electric dehydrators of the oil treatment plant (OTP). In OTP at a temperature of about 120 ° C and in the presence of demulsifiers, the water content (less than 1% of mass), mineral salts (up to 20-300 mg/l) are reduced, and the third-stage separation gas is released. Stabilized oil (4) is supplied to the crude oil delivery unit (CODU) and sent to the refinery via the main oil pipeline. Water from OTP and water from pre-discharge tanks is transferred to the water processing unit (WPU). Purified water (5), as a rule, is used to flood the formation (injection into the reservoir). Gases separated in the separators are piped to the gas processing plant (GPP) for separation [3].

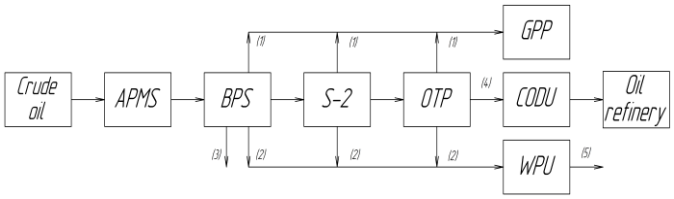


Fig. 1. The scheme for oil collecting and treatment in the fields

An OTP unit can be conditionally represented in the form of a scheme:

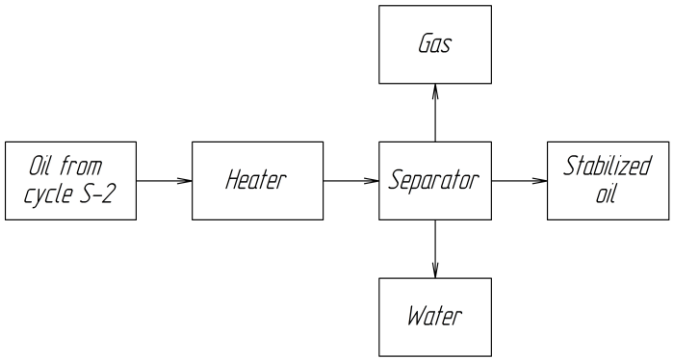


Fig. 2. Classical scheme of oil separation in OTP unit

The authors propose an improved separation scheme [4] in the OTP unit, designed to optimize power consumption by increasing the efficiency of the separator plant by means of using the heat released in the rotor drum, conductors and the stator magnetic circuit. In the classical scheme of separation (Fig. 2), the oil is heated to the set temperature in the preheater. Fig. 3 is a scheme of a separator unit made according to the classical scheme.

We can see from Fig. 3 that the separator drum 1 fixed to the shaft 2 is driven by the motor 4 through the clutch 3 and the reduction gear. The crude oil is preheated in the preheater 5 and is fed through the connecting pipe 6 to the separator drum 1. With this separation scheme, the energy is supplied to the asynchronous motor 4 (consisting of such main parts as the stator core with the stator winding and the rotor) and the heater 5. It should be noted that, operation of asynchronous motor 4 causes irreversible energy losses in the form of heat release in the main parts of the engine, namely: in the stator magnetic circuit, in the stator winding, in the rotor.

In the improved separation scheme (Figure 4), the oil preheating process is carried out in the preheater, in the separator drum – in the rotor, stator. This reduces the cost of oil heating.

Fig. 5 shows the design of oil separation unit based on a separator engine (SE).

The oil separation unit comprises: a separator body 1, an electric motor stator mounted therein, consisting of two parts (a cylindrical part 2-1, an axial part 2-2), with a winding 3 of two stator parts; the tubes 4 are installed around the frontal parts, filled with compound 5; the separator drum 6, which is simultaneously the motor rotor, rigidly connected to the axis 7, the axis 7 is installed in the bearing supports 8 and 9. The drum of the separator 6 consists of a base 10 with a central tube, dividing trays 11, a cover 12, a tray-holder 13, a retaining ring 14. The connection tube 16 connects the oil preheater 15 to the inlet of the tubes 4, and the connection tube 17 connects the outlet of the tubes 4 to the interior of the separator drum 6.

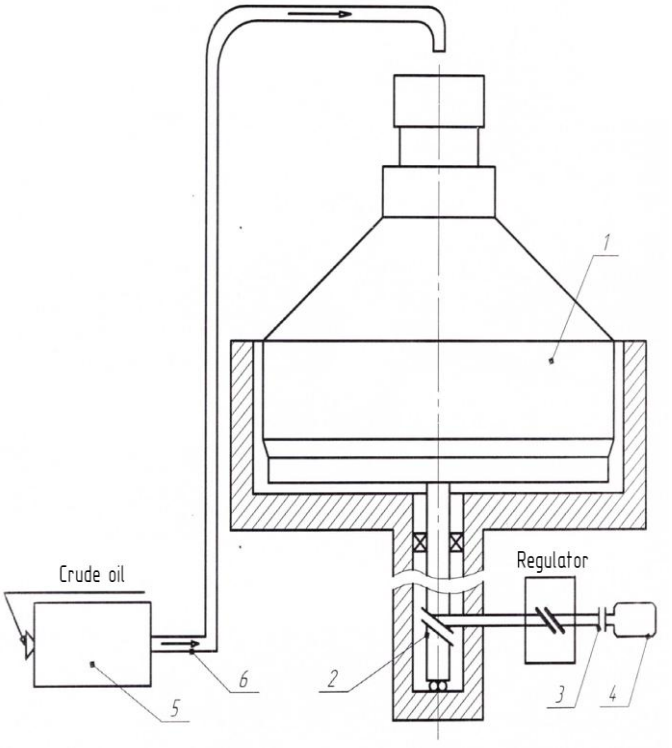


Fig. 3. Classical oil separation unit

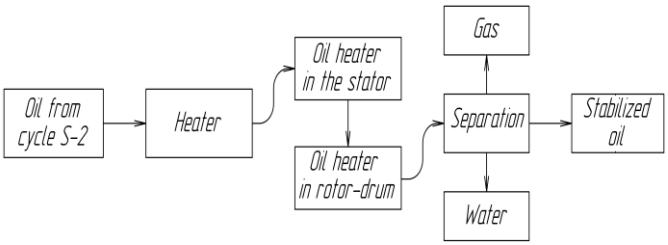


Fig. 4. Improved separation scheme

Fig. 5 shows a photograph of a model installation made according to the SE scheme.

The authors carried out a study of the energy efficiency of the proposed separation scheme [5].

It seems expedient to improve the engine-separator to determine the most heated area of the machine in order to

increase the complex efficiency of the installation. For this purpose, a mathematical modeling of the temperature field of the separator motor was carried out.

There are known works [6-10] related to the calculation of the thermal regimes of electric machines, including those based on the construction of partial equations system that take thermal processes into account in various parts of the machine. To calculate the thermal conditions of SE machine, the machine must be represented schematically (see Figure 7) by an approximate physical model of the machine engine (more specifically, SE) in which the smooth massive rotor is the working member where the product flows, and which is simultaneously a refrigerant. The frontal parts of the stator winding and the outer part of the stator core are wrapped in a pipeline through which the product flows (refrigerant). The arrows in Fig. 7 show schematically the motion of the liquid.

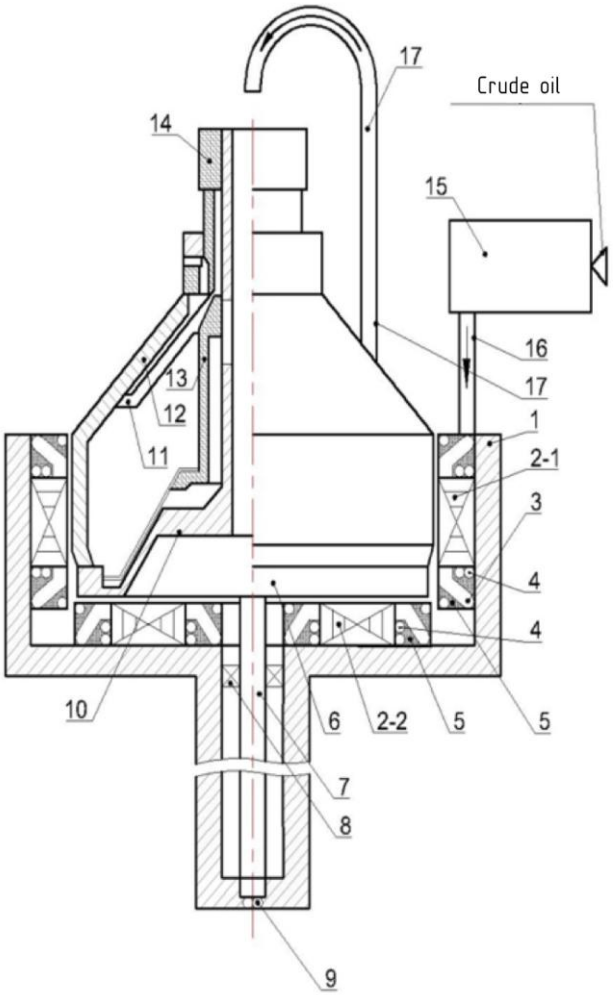


Fig. 5. Oil separation unit

Fig. 6. The working model of the oil separation unit

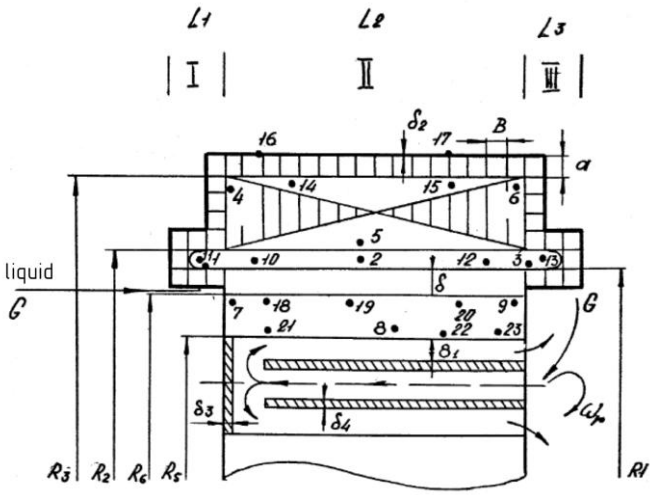


Fig. 7. Asynchronous motor with variable parameters, as a basic SE model for the study of thermal transients

To calculate the SE thermal regime of D-C, let us propose a system of equations (1).

$$
\begin{gathered}
C_{\text{м}}\rho_{\text{м}}\frac{\partial T_{s1}}{\partial t}=\lambda_{\text{м}r}\ \frac{\partial^2 T_{s1}}{\partial r^2}+\frac{1}{r}\frac{\partial T_{s1}}{\partial r}\ +\ \frac{\partial^2 T_{s1}}{\partial Z^2}\ \lambda_{\text{м}z}+\frac{R_{s1}}{V_{s1}}\ i_{s1\mathcal{L}}^2+i_{s1\beta}^2+i_{s1\gamma}^2\ ;\\
R_1\le r\le R_2,\ \ 0\le Z\le L_5;\\
C_s\rho_s\frac{\partial T_{s2}}{\partial t}=\lambda_{sr}\ \frac{\partial^2 T_{s2}}{\partial r^2}+\frac{1}{r}\frac{\partial T_{s2}}{\partial r}\ +\ \frac{\partial^2 T_{s2}}{\partial Z^2}\ \lambda_{sz}+\frac{R_{s2}}{V_{s2}}e^{r\ \sqrt{2\mu_s\gamma_{s2}f_0}}\ i_{s2\mathcal{L}}^2+i_{s2\beta}^2+i_{s2\gamma}^2\ ;\\
R_2\le r\le R_3,\ \ L_1\le Z\le L_2\\
C_r\rho_r\frac{\partial T_r}{\partial t}=\lambda_r\ \frac{\partial^2 T_r}{\partial r^2}+\frac{1}{r}\frac{\partial T_r}{\partial r}\ +\ \frac{\partial^2 T_r}{\partial Z^2}\ +\frac{R_r}{V_r}e^{r\ \sqrt{2\mu_r f_0 S\gamma_r}}\ i_{r\mathcal{L}}^2+i_{r\beta}^2+i_{r\gamma}^2\ ;\\
R_5\le r\le R_6,\ \ L_1\le Z\le L_2
\end{gathered}
\qquad (1)
$$

where $i_{s1\mathcal{L}}$, $i_{s1\beta}$, $i_{s1\gamma}$, $i_{s2\mathcal{L}}$, $i_{s2\beta}$, $i_{s2\gamma}$, $i_{r\mathcal{L}}$, $i_{r\beta}$, $i_{r\gamma}$ – , respectively, the currents in the stator and rotor windings along axes $\mathcal{L}, \beta, \gamma$ ;

$R_{s1}, R_{s2}, R_r$ - an active resistance of stator and rotor windings along axes, $\mathcal{L}, \beta, \gamma$, which respectively depend on temperatures $T_{s1}, T_{s2}, T_r$;

$\mathcal{J}$ - inertia moment;

S - sliding motion;

P - number of pairs of poles;

$\omega_r$ - angular rotational speed of the rotor-drum;

$\mu_s, \mu_r$ - relative magnetic permeability of stator core and rotor core steel;

$C_{\text{м}}, C_s, C_r$ - specific heat of the winding of the stator phase, stator core and rotor;

$\rho_{\text{м}}, \rho_s, \rho_r$ - densities of the stator phase coil material, stator core and rotor;

$\lambda_{\text{мг}}, \lambda_{\text{мz}}, \lambda_{sr}, \lambda_{sz}, \lambda_r$ - thermal conductivity coefficients of the winding of the phase and the stator core along the axes and the rotor;

r, z - cylindrical coordinates;

t - time;

$f_0$ - utility frequency;

$T_{s1}, T_{s2}, T_r$ - instantaneous temperatures;

$\gamma_{s1}, \gamma_r$ - conductivity of the material, which are temperature-dependent;

$V_r, V_{s1}, V_{s2}$ - volume of the studied machine node

Index "S1" corresponds to the windings of the stator phases, index "S2" - to the stator windings, through which equivalent eddy currents flow; "R" is the rotor.

The above mathematical model will be incorrect without recording of the boundary conditions.

Actually, the boundary conditions between different machine nodes, the product (coolant) and the environment are determined by the known heat transfer rules [11-14].

So, on the boundary "the groove of the winding - the stator core" - the boundary conditions are of the fourth kind.

At the boundary "stator core - coolant and machine nodes - environment" - boundary conditions are of the third kind.

On the basis of the foregoing, the boundary conditions are given in (2).

The coefficient of thermal conductivity of the stator winding $\lambda_{\text{мг}}$, $\lambda_{\text{мz}}$ is determined by known formulas, as an equivalent coefficient of thermal conductivity $\lambda_{\text{м}}$ of the streamlined windings of circular cross-section wires.

The value $\lambda_{\text{м}}$ depends on the diameter of the wire and the thickness of its insulation, on the layout of the winding in the groove, on the coefficients of wire thermal conductivity, on the insulation and insulating pads.

$$
\begin{gathered}
\lambda_{\text{мг}} \frac{\partial T_{s1}(r,z,t)}{\partial r}_{r=R_2} = \lambda_{sr} \frac{\partial T_{s2}(r,z,t)}{\partial r}_{r=R_2}, \\
T_{s1}(r,z,t)_{r=R_2} = T_{s2}(r,z,t)_{r=R_2}, \\
L_1 \le Z \le L_2; \\
\lambda_r \frac{\partial T_r\ r,z,t}{\partial r}_{r=R_5} = \lambda_{\text{мг}} \frac{\partial T_{s1}\ r,z,t}{\partial r}_{r=R_1} = \mathcal{L}_{13}\ \omega_r\ \ T_r - T_{s1} \\
L_1 \le Z \le L_2; \\
\lambda_r \frac{\partial T_r\ r,z,t}{\partial r}_{r=L_1} = \lambda_r \frac{\partial T_r\ r,z,t}{\partial r}_{z=L_2} = \mathcal{L}_{14}\ \omega_r\ \ T_r - T_0\ , \\
R_5 \le r \le R_6; \\
\lambda_f \frac{\partial T_{f6}\ z,t}{\partial Z}_{z=L_1} = \mathcal{L}_5\ \omega_r, r\ \ T_{f10} - T_0\ , \\
0 \le r \le R_5; \\
S_f C_f \rho_f\ \ \frac{\partial T_{f1}}{dt} + V_f \frac{\partial T_{f1}}{dZ}\ = \mathcal{L}_1 \Pi_1\ T_{s1} - T_{f1}\ + \mathcal{L}_2 \Pi_2\ T_{f1} - T_0\ , \\
R_1 \le r \le R_2,\ \ 0 \le Z \le L_1,\ \ T_0 = T_{f1})_{z=0}; \\
T_{f1}\ _{z=L_1} = T_{f2}\ _{z=L_1}; \\
S_f C_f \rho_f\ \ \frac{\partial T_{f2}}{dt} + V_f \frac{\partial T_{f2}}{dZ}\ = \mathcal{L}_3 \Pi_3\ \ T_{s2}\ _{z=L_1} - T_{f2}\ + \mathcal{L}_4 \Pi_4\ T_{\text{ж}2} - T_0\ , \\
R_3 \le r \le R_2; \\
T_{f2}\ _{z=L_1} = T_{f3}\ _{z=L_1}; \\
S_f C_f \rho_f\ \ \frac{\partial T_{f3}}{dt} + V_f \frac{\partial T_{f3}}{dZ}\ = \mathcal{L}_{12} \Pi_5\ \ T_{s2}\ _{r=R_3} - T_{f3}\ + \mathcal{L}_6 \Pi_6\ T_{f3} - T_0\ , \\
L_1 \le Z \le L_2; \\
T_{f3}\ _{z=L_2} = T_{f4}\ _{z=L_2}; \\
S_f C_f \rho_f\ \ \frac{\partial T_{f4}}{dt} + V_f \frac{\partial T_{f4}}{dZ}\ = \mathcal{L}_3 \Pi_7\ \ T_{s2}\ _{Z=L_2} - T_{f4}\ + \mathcal{L}_8 \Pi_8\ T_{f4} - T_0\ ; \qquad (2) \\
R_3 \le r \le R_2; \\
T_{f4}\ _{z=L_2} = T_{f5}\ _{z=L_2}; \\
S_f C_f \rho_f\ \ \frac{\partial T_{f5}}{dt} + V_f \frac{\partial T_{f5}}{dZ}\ = \mathcal{L}_9 \Pi_9\ T_{s1} - T_{f5}\ + \mathcal{L}_{10} \Pi_{10}\ T_{f5} - T_0\ ; \\
L_2 \le Z \le L_3; \\
R_1 \le r \le R_2; \\
T_{f5}\ _{z=L_3} = T_{f6}\ _{z=L_1}; \\
S_f C_f \rho_f\ \ \frac{\partial T_{f6}}{dt} + V_f \frac{\partial T_{f6}}{dZ}\ = \mathcal{L}_{11}\ \omega_r, z\ \cdot\ T_r\ _{r=R_5} - T_{f6}\ , \\
L_1 \le Z \le L_2; \\
\lambda_{c2r} \frac{\partial T_{s2}(r,z,t)}{\partial Z}_{r=R_3} = \mathcal{L}_{12}\ T_{s2} - T_{f3}\ , \\
L_1 \le Z \le L_2; \\
\lambda_{c2z} \frac{\partial T_{c2}(r,z,t)}{\partial Z}_{z=L_1} = \mathcal{L}_8\ T_{c2} - T_{f2}\ , \\
R_2 \le r \le R_3; \\
\lambda_{c2z} \frac{\partial T_{c2}(r,z,t)}{\partial Z}_{z=L_2} = \mathcal{L}_7\ T_{c2} - T_{f4}\ , \\
R_2 \le r \le R_3; \\
\lambda_r \frac{\partial T_r(r,z,t)}{\partial r}_{r=R_5} = \mathcal{L}_{11}\ \omega_r, z\ \ T_r - T_{f6}\ , \\
L_1 \le Z \le L_2; \\
\lambda_{\text{мг}} \frac{\partial T_{c1}(r,z,t)}{\partial r}_{r=R_2} = \lambda_{\text{мг}} \frac{\partial T_{c1}(r,z,t)}{\partial r}_{r=R_1} = \lambda_{\text{мг}} \frac{\partial T_{c1}(r,z,t)}{\partial r}_{z=0} = \mathcal{L}_1\ T_{c1} - T_{f1}\ , \\
0 \le Z \le L_1,\ \ R_1 \le r \le R_2; \\
\lambda_{\text{мг}} \frac{\partial T_{c1}(r,z,t)}{\partial r}_{r=R_2} = \lambda_{\text{мг}} \frac{\partial T_{c1}(r,z,t)}{\partial r}_{r=R_1} = \lambda_{\text{мz}} \frac{\partial T_{c1}(r,z,t)}{\partial z}_{z=L_3} = \mathcal{L}_9\ T_{s1} - T_{f5}
\end{gathered}
$$

$$
\lambda_{\text{мг}} \frac{\partial T_{c1}(r,z,t)}{\partial r}_{r=R_2} = \lambda_{\text{мг}} \frac{\partial T_{c1}(r,z,t)}{\partial r}_{r=R_1} = \lambda_{\text{мz}} \frac{\partial T_{c1}(r,z,t)}{\partial z}_{z=L_3} = \mathcal{L}_9\ T_{s1} - T_{f5}
$$

where $C_{\text{fi}}$, $p_{\text{fi}}$ - specific heat and fluid density;

$V_{\text{f}}$- velocity of fluid flow in the channel;

$\mathcal{L}_1, \mathcal{L}_2, \mathcal{L}_3, \mathcal{L}_4, \mathcal{L}_6, \mathcal{L}_7, \mathcal{L}_8, \mathcal{L}_9, \mathcal{L}_{10}, \mathcal{L}_{12}, \mathcal{L}_{13}$ - heat transfer coefficients;

$\mathcal{L}_5, \mathcal{L}_{11}, \mathcal{L}_{14}$ - heat-conduction coefficients;

$S_f$ - fluid passage cross-section;

$\Pi_1, \ldots, \Pi_{10}$ - perimeters of thermal contact between surface and liquid;

$T_{f1} \ldots, T_{f6}$ - instantaneous fluid temperatures.

The coefficient of thermal conductivity of the laminated packages across the sheets ($\lambda_{sz}$) is determined by calculation and depends on the thickness of the steel sheet and the insulation between the sheets, on the thermal conductivity of the steel and insulation.

The coefficients of thermal conductivity of the rotor material ($\lambda_r$) and the electrical steel of the stator pack along the sheets ($\lambda_{sr}$) are determined from the reference data.

Specific heat capacities and liquid density, the rotor and stator core materials are selected by reference.

The specific heat of the stator winding $C_м$ is defined as the equivalent heat capacity

$$C_{eq} = C_м = \ C_{cop}V_{cop} + C_aV_a + C_{i3}V_{i3} \ /V,$$

where $C_{cop}, C_a, C_{i3}$ - specific heat of copper, air, insulation;

$V_{cop}, V_a, V_{i3}$ - the volume occupied by copper wires, air, insulation in the total volume V.

The above-stated model by (1) (2) causes implementation difficulties.

During the simulation, the COMSOL Multiphysics software was selected by the authors to optimize the power consumption of the OTP unit [15]. The COMSOL Multiphysics software is based on advanced numerical methods, and is a universal software platform for computer simulation of physical tasks. COMSOL Multiphysics software allows us to take into account related or "multi-physical" phenomena. Additional interfaces provide the use of modeling in the package COMSOL Multiphysics in technical calculations, CAD system and automation design of electronic devices. COMSOL Multiphysics® also includes the COMSOL® API for use with Java®, which adds additional COMSOL Multiphysics® integration capabilities to other applications: MatLab, Excel, SolidWorks, Inventor, AutoCAD, Revit, Creo Parametric, Pro / E, Solid Edge , CATIA [16].

When modeling the temperature field, the separator was conditionally represented by the model under study shown in Fig. 8. In Fig. 8, position I replaces positions 2-1 of the actual separator in Fig. 5, position II replaces position 2-2 of the actual separator in Fig. 5, position III replaces position 6 of the actual separator in Fig. 5, position IV replaces position 4 of the actual separator in Fig. 5. With such a replacement, the following assumptions were made: the rotor - the separator drum is presented as a hollow cylinder inside which a tube with a circulating liquid is located, the stator winding is taken as an integrated wreath. During the mathematical experiment, different sizes of separators were used (see Table 1). In the numerical experiment, the following initial conditions were accepted: t0=20 C° (293.15 K)$t_0 = 20^{\circ}$. The feed rate of the tested liquid is determined by the appropriate type of separator and by its design features for feeding the product to be separated. Oil heating in the stator and rotor is given in accordance with the calculations given in [5].

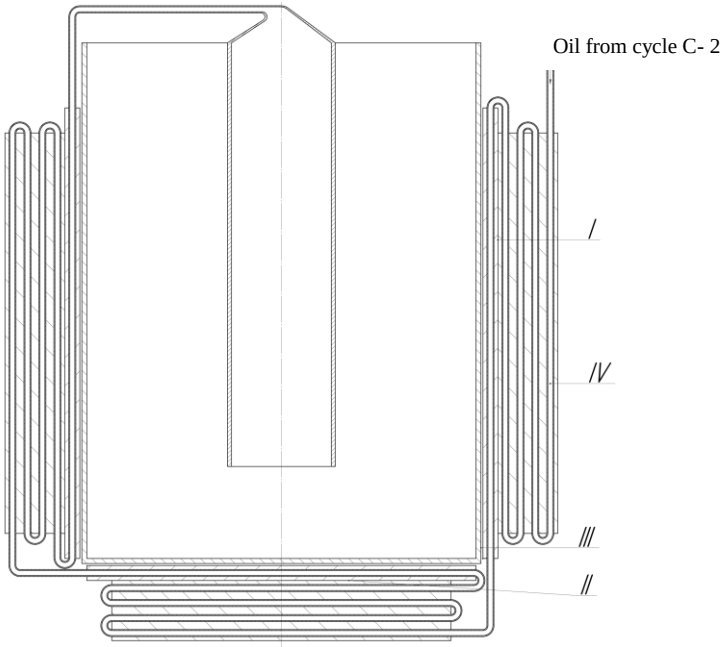


Fig. 8. Design model of the motor-separator

At the end of mathematical modeling in the COMSOL Multiphysics software, a picture of the thermal field of the machine was obtained.

Fig. 9-12 present the results of a mathematical experiment in the form of screenshots.

Figure 9 shows a screenshot of the thermal field of the engine-separator. Taking into account the temperature scale presented in the right-hand part in Fig. 8 (in Kelvins), it is possible to determine the temperature of individual parts of the engine design - the separator represented by the calculation model in Fig. 8. As one can see from Fig. 9, the most heated area of the engine-separator construction is a rotor-drum. Fig. 9 also shows the process of heating the starting product in the separator motor.

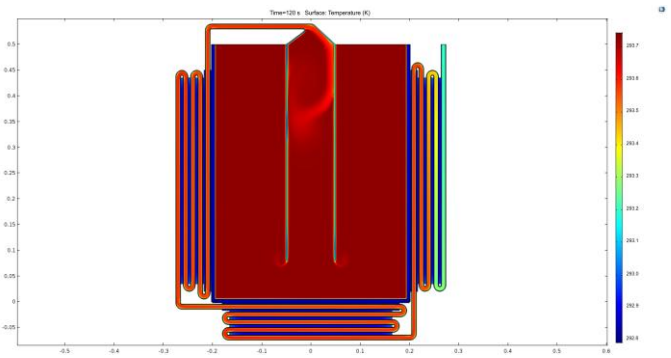

Fig. 9. Screenshot of the thermal field of the engine-separator (drum type SL-1)

Mathematical modeling of temperature field construction for the separator engine was carried out for three standard sizes of real separators, the main technical data of which are given in Table 1.

TABLE I. THE MAIN PARAMETERS OF THE INVESTIGATED SEPARATORS

| | Separator type | | |
|---|---|---|---|
| | ***SL-1*** | ***SL-3*** | ***SL-5*** |
| Separator efficiency, Q ($m^3$/h) | 2.45 | 5.75 | 12,5 |
| Rated power of separator engine, (kW) | 2.2 | 5.5 | 15 |

Fig. 10-12 show screenshots of temperature dependences of individual parts of the separator engine design as a function of time. In the above figures, the time (in seconds) is plotted along the abscissa, and the temperature (in Kelvins) along the ordinate axis.

The graphs, shown in dark blue (Sensor 1), show the time variation in the oil temperature before entering the tubes that run around the stator end of the separator motor. The graphs, shown in green (Sensor 2), show the time variation in the oil temperature at the exit of the tubes that run around the end of the stator of the separator motor into the tubes that run around the cylindrical part of the stator of the separator motor. The graphs, shown in black (Sensor 3), show the time variation in the oil temperature before entering the rotor drum. The graphs, shown in red (Sensor 4), show the time variation in the oil temperature at the exit from the rotor-drum.

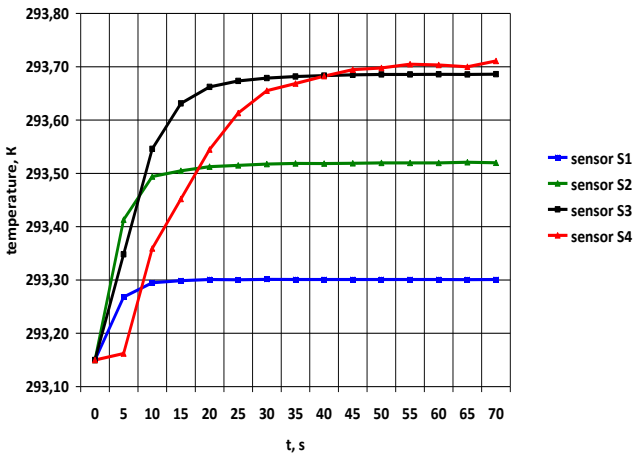


Fig. 10. Graph of mathematical modeling results for separator motor (drum type SL-1)

Table 2 shows the calculating results of the stator and drum-rotor heating for the separator motor.

TABLE II. CALCULATION RESULTS

| Separator type | $\Delta t_{st}$ | $\Delta t_r$ | $t_\Sigma$ |
|---|---|---|---|
| SL-1 | 0,53 | 0,05 | 0,58 |
| SL -3 | 0,38 | 0,02 | 0,4 |
| SL -5 | 0,42 | 0,015 | 0,435 |

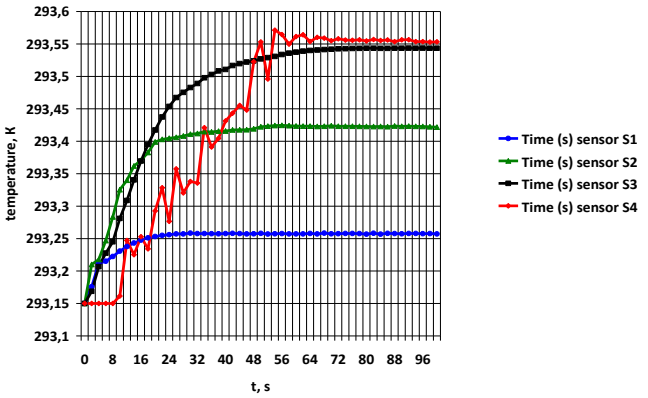


Fig. 11. Graph of mathematical modeling results for separator motor (drum type SL-3)

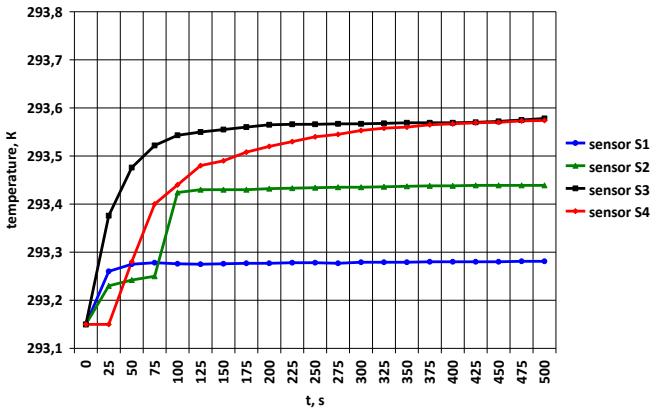


Fig. 12. Graph of mathematical modeling results for separator motor (drum type SL-5)

## III. CONCLUSION

Thus, the use of the combined design of separator units (engine-separator) will reduce the energy consumption, and calculation of the temperature field will allow one to determine the machine with the greatest heat transfer using the design.

## *References*

[1] VN Erich, MG Rasina, MG Rudin, Chemistry and technology of oil and gas. Ed. 2 nd, trans. L., "Chemistry", 1977, p. 424.

[2] LP Mstislavskaya, MF Pavlinich, VP Filipov, Fundamentals of oil and gas production: Textbook. FSUE Publishing House "Oil and Gas" of the Russian State University of Oil and Gas. Afte rIM Gubkin, 2 nd ed. Corrected and added, 2003, p. 276.

[3] OF Glagoleva, V.M. Kapustin, Oil refining technology. In 2 parts. Part one. Primary processing of oil, Moscow: Chemistry, Kolos S, 2007, p. 400.

[4] LE Kopelevich, Method of oil separation, Pat. No 2585636 of the Russian Federation, No. 2015110413/05; Claimed. 2015-03-23; Publ. May 27, 2016, Bul. № 15.

[5] B Kh. Gaitov, YaM Kashin, LE Kopelevich, AV Samorodov, VA Kim "Installation for oil separation," Oil Industry, No. 7, pp. 90-92, 2017.

[6] ELCUT. Simulation of two-dimensional fields by the finite element method. Version 5.2. PC "TOP", St. Petersburg, 2005.

[7] MV Sochava, Improvement of engineering methods for calculating the thermal inertia of active parts of powerful electric machines: PhD thesis, S.-Petersburg. Polytechnical. University, St. Petersburg, 2008, p. 141.

[8] IN Zheleznyak, Mathematical modeling of thermal fields in the active zone of electric machines with indirect water cooling: PhD thesis: St-Petersburg. Polytechnical. University, St. Petersburg, 2010, p. 139.

[9] GG Schastliviy, Heating of closed asynchronous motors, Kiev: Naukova Dumka, 1966, p. 196.

[10] GG Schastliviy, Uneven heat dissipation and heating of the end parts of highly used alternating current machines: Dis .... kand. ... Doct. Tech. Sciences, Kiev, 1973, p. 459.

[11] AV Lykov, Theory of heat conduction. M., Higher School, 1967, p. 599.

[12] ME Mamedshahov, "On the use of nonlinear boundary values in the study of thermal processes in electric machines," Electricity, No. 10, pp. 22-26, 1981.

[13] ME Mamedshahov, "Calculation of the characteristics of electromechanical energy converters taking into account the temperature change," Elektrichestvo, no. 3, pp. 64-66, 1984.

[14] ME Mamedshahov, "A Refined Method for the Thermal Calculation of Coupled Knots of Electric Machines," Electricity, № 12, pp. 41-43, 1982.

[15] Demo version of COMSOL Multiphysics software package. Retrieved from: https://www.comsol.com/request-a- demo (accessed date 12.05.17).

[16] COMSOL. Retrieved from: https://www.comsol.ru/comsol-multiphysics (accessed date 12.05.17).